DOI: 10.26599/FSHW.2026.9251178

Contents lists available at SciOpen

Food Science and Human Wellness

journal homepage: https://www.sciopen.com/journal/2097-0765

China Food Publishing Co.

Lactoferrin Hydrolysate Mitigates Azoxymethane/Dextran Sulfate Sodium–Induced Colon Cancer by Modulating Gut Microbiota and Microbial Metabolites

Hanjun Jiang [1], Xue Deng [1], Jing Yang [2], Patangal Basak [1], Huayi Suo [1], and Jiajia Song [1, *]

[1] *College of Food Science, Southwest University, Chongqing 400715, China*

[2] *School of Food Science and Engineering, Chongqing Technology and Business University, Chongqing 400067, China*

ABSTRACT: Colon cancer is one of the most common malignant tumors worldwide and is associated with high morbidity and mortality. Conventional treatments are typically administered at advanced stages and often lead to severe adverse effects. Therefore, developing safe and effective nutritional interventions from natural food sources is of great importance for the prevention and management of colon cancer. Dairy-derived protein hydrolysates have received increasing attention as functional food components due to their biological activities and favorable safety profiles. In this study, lactoferrin (LF) was hydrolyzed using alkaline protease to obtain lactoferrin hydrolysate (LFH). LFH was administered to mice with azoxymethane/dextran sulfate sodium-induced colon cancer to evaluate its protective effects. LFH markedly alleviated colonic tissue injury, reduced serum levels of pro-inflammatory cytokines IL-1β, IL-6, and TNF-α, and decreased the expression of tumor markers CEA, CA19-9, as well as the proliferation marker Ki-67, thereby inhibiting tumor progression. At the molecular level, LFH downregulated key genes in the Wnt/β-catenin pathway, including c-Myc, β-catenin, and Cyclin D1. Furthermore, LFH upregulated pro-apoptotic genes Bax, caspase-9, caspase-3, and p53, while downregulating anti-apoptotic genes Bcl-2 and Bcl-xl, suggesting enhanced apoptotic responses in tumor cells. LFH also significantly improved gut microbiota composition by reducing harmful bacteria such as *Bacillus*, *Enterorhabdus*, and *Odoribacter*, while increasing beneficial genera including *Ruminococcus* and *Eubacterium_siraeum_group*. Correspondingly, LFH elevated several gut microbial metabolites such as Chrysogine, Agmatine, 5′-Deoxy-5-Fluorocytidine, and Glutamyl-γ-Glutamate. Overall, this study provides new insights into the biological effects of LFH on colon cancer and supports its potential application in the development of LFH-based functional foods.

Keywords: Lactoferrin, Protein hydrolysate, Colon cancer, Gut microbiota, Microbial metabolites

1. Introduction

Colon cancer is one of the major malignant tumors worldwide and is characterized by high morbidity and mortality. According to the latest GLOBOCAN 2022 estimates from the International Agency for Research on Cancer (IARC) of the World Health Organization (WHO), colorectal cancer is the third most commonly diagnosed malignancy worldwide, with 1.93 million new cases and approximately 900,000 deaths reported in 2022. Although colorectal cancer includes both colon and rectal tumors, colon cancer accounts for a substantial proportion of the global disease burden. Current treatment strategies for colon cancer include

***Corresponding author**
jiajias@swu.edu.cn (H. J. Jiang).

Received 3 September 2025
Received in revised from 11 November 2025
Accepted 5 February 2026

radiotherapy, chemotherapy, surgery, immunotherapy, and targeted therapy; however, these approaches are primarily applied in advanced stages and are often associated with severe adverse effects such as fatigue, alopecia, and hepatic or renal toxicity [1, 2]. Food-derived bioactive compounds—including polyphenols, polysaccharides, and protein peptides—have demonstrated therapeutic potential in alleviating gut-related disorders such as inflammatory bowel disease (IBD), colitis, and colon cancer [3-5]. Among these, protein peptides have shown notable promise in mitigating colon cancer. For example, walnut protein peptides induce apoptosis in colon cancer cells by activating cysteine-aspartic acid protease (caspase)-3, inhibit matrix metalloproteinase-9 (MMP9) to prevent metastasis, and suppress cell proliferation, thereby exerting anti-colon-cancer effects [6]. Camel whey protein hydrolysates inhibit the growth of human colorectal cancer HCT116 cells by inducing G2/M cell cycle arrest. This effect is associated with decreased cyclin-dependent kinase 1 (CDK1) and Cyclin B1 expression, increased phosphorylated CDK1 (p-CDK1) and phosphorylated histone H3 (p-histone H3) levels, and modulation of cyclin-dependent kinase inhibitor 1 (p21) and tumor protein p53 (p53) [7]. In azoxymethane/dextran sulfate sodium (AOM/DSS)-induced mouse models, quinoa protein hydrolysate alleviates colon cancer by inhibiting histone deacetylase (HDAC1), regulating cancer-related factors such as nuclear factor (NF)-κB, interleukin (IL)-6, IL-8, B-cell lymphoma 2 (Bcl-2), and caspase-3, and restoring gut microbial balance and short-chain fatty acid levels [8, 9]. These findings highlight the potential of food-derived protein peptides as nutritional interventions for colon cancer.

Lactoferrin (LF) is an iron-binding glycoprotein widely distributed in mammalian milk and other secretions. It exhibits diverse biological functions, including antibacterial, antiviral, immunomodulatory, and anti-inflammatory activities [10, 11]. However, the relatively high molecular weight of intact LF may limit its bioavailability. In contrast, lactoferrin hydrolysate (LFH), produced through enzymatic hydrolysis, retains the essential bioactive domains of LF while exhibiting enhanced absorption, solubility, and bioavailability due to its reduced molecular size [12]. Previous studies have shown that LFH exerts antihypertensive and anti-inflammatory effects by inhibiting angiotensin-converting enzyme (ACE) and regulating inflammation-associated pathways [13]. LFH prepared from camel LF demonstrated ACE inhibitory activity up to 89.1%, significantly higher than that of native LF, suggesting enhanced antihypertensive potential [14]. *In vivo*, LFH inhibits ACE- and endothelin converting enzyme (ECE)-dependent vasoconstriction, thereby exerting antihypertensive effects in spontaneously hypertensive rats [15]. Despite these findings, its therapeutic efficacy against colon cancer has not been previously reported.

In this study, colon cancer was induced in mice using the AOM/DSS model. By evaluating body weight changes, colon length, histopathological features, serum biochemical markers, and tumor-related indices, we examined the protective effects of LFH. We further analyzed the expression of genes related to the wingless/integration site β-catenin (Wnt/β-catenin) pathway and apoptosis, as well as alterations in gut microbiota and microbial metabolites, to clarify how LFH contributes to the alleviation of colon cancer. This study provides a theoretical basis for the development of LFH-based functional foods aimed at colon cancer prevention or relief.

2. Materials and methods

2.1 Materials

AOM was purchased from Sigma-Aldrich (St. Louis, MO, USA). DSS was obtained from MP Biomedicals Inc. (Irvine, CA, USA). LF (purity >98%) was sourced from Beston Global Food Company (Adelaide, Australia). Alkaline protease (≥200,000 U/g) was obtained from Beijing Solarbio Science & Technology Co., Ltd. (Beijing, China). Ki-67 antibody (GB121141), Cyclin D1 antibody (GB151372), β-catenin antibody (GB12015), horseradish peroxidase (HRP)-labeled goat anti-mouse IgG (H+L) (GB23301), Cy3-labeled goat anti-rabbit IgG (H+L) (GB21303), Cy3-labeled goat anti-mouse IgG (H+L) (GB21301), 3,3'-diaminobenzidine (DAB) chromogenic kit, EDTA antigen retrieval solution, bovine serum albumin (BSA), 4',6-diamidino-2-phenylindole (DAPI) staining solution, autofluorescence quencher, and fluorescence quencher were purchased from Wuhan Servicebio Technology Co., Ltd. (Wuhan, Hubei, China). Paraformaldehyde fixative, Trizol reagent, and RevertAid First Strand cDNA Synthesis Kit were obtained from Thermo Fisher Scientific (Waltham, MA, USA).

2.2 Preparation of LFH

LF was hydrolyzed using alkaline protease. LF powder was dissolved in deionized water, and alkaline protease was added at 5% (w/w). The mixture was incubated at 50℃ and pH 11.0 for 4 h with continuous stirring. Enzyme inactivation was performed by heating at 85℃ for 20 min. After centrifugation, the supernatant was collected, neutralized, freeze-dried, and stored for subsequent analysis.

2.3 Construction of animal models and sample collection

Male C57BL/6J mice (6-7 weeks old) were purchased from Hunan SJA Laboratory Animal Co., Ltd. (Changsha, Hunan, China) and housed in a specific-pathogen-free (SPF) facility under controlled environmental conditions (24-26℃, 50-60% humidity, 12 h light/dark cycle). Mice were allowed one week of acclimatization. All procedures were approved by the Laboratory Animal Welfare Ethics Review Committee of Southwest University (IACUC-20241125-09, Chongqing, China).

The AOM/DSS-induced colon cancer model was established as previously described by Wei et al., with minor modifications [16]. A total of 24 mice were randomly assigned to three groups: control, AOM/DSS, and AOM/DSS+LFH (n = 8 per group). Mice in the control group received a single intraperitoneal injection of 0.9% saline, followed by daily oral gavage of 0.9% saline and access to regular drinking water. Mice in the AOM/DSS group received a single intraperitoneal injection of AOM (10 mg/kg·bw). One week later, the mice were given 2% (w/v) DSS in their drinking water for one week, followed by two weeks of normal drinking water. This cycle was repeated three times, resulting in a 12-week experimental period. Mice in the AOM/DSS+LFH group underwent the same AOM/DSS induction protocol and additionally received a daily oral dose of LFH (400 mg/kg·bw) beginning on the day of AOM administration. Body weight was recorded weekly. At the end of the experiment, fecal, serum, and colonic tissue samples were collected and stored at -

80℃. No animals died unexpectedly or failed to develop tumors; therefore, no subjects were excluded. Investigators responsible for sample analysis were blinded to group allocation.

2.4 Pathological analysis of colonic tissue

Colonic tissues were fixed in 4% paraformaldehyde, embedded in paraffin, and sectioned. Hematoxylin and eosin (H&E) staining was performed following standard procedures. Morphological changes were observed and imaged using a light microscope (Olympus, Tokyo, Japan).

2.5 Serum biochemical determination

Serum biochemical markers were quantified using enzyme-linked immunosorbent assay (ELISA) kits (Jiangsu Meibiao Biotechnology Co., Ltd., Yancheng, China). A one-step sandwich ELISA based on a double-antibody detection system was performed according to the manufacturer's instructions. Microplate wells were pre-coated with capture antibodies specific for mouse IL-1β, IL-6, tumor necrosis factor (TNF)-α, arcinoembryonic antigen (CEA), and carbohydrate antigen 19-9 (CA19-9). Samples, standards, and HRP-conjugated detection antibodies were added sequentially. After incubation and washing, tetramethylbenzidine (TMB) substrate was added. The HRP-catalyzed chromogenic reaction yielded a blue color, which turned yellow upon acidification. Absorbance was measured at 450 nm, and analyte concentrations were calculated from standard curves.

2.6 Immunohistochemical analysis of Ki-67

Immunohistochemistry was performed following a modified version of Liu's method [17]. Paraffin-embedded colonic tissue sections were incubated overnight at 4℃ with Ki-67 antibody (1:300), followed by incubation with HRP-labeled goat anti-mouse IgG (H+L) (1:200). DAB was used for chromogenic development, and hematoxylin was used for nuclear counterstaining. Ki-67-positive cells were observed using a microscope (Olympus, Tokyo, Japan). Quantification was performed with Image-Pro Plus 6.0 (Media Cybernetics Inc., USA), and the percentage of Ki-67-positive cells was calculated.

2.7 Quantitative real-time PCR (qRT-PCR)

Total RNA was extracted from colonic tissues using Trizol reagent and reverse transcribed into cDNA. Equal amounts of cDNA were used for qRT-PCR with SYBR Green Master Mix on a qRT-PCR detection system. PCR conditions were as follows: 95℃ for 20 s, 60℃ for 20 s, 72℃ for 30 s, repeated for 40 cycles. GAPDH served as the internal reference gene. Relative gene expression was calculated using the $2^{-\triangle\triangle CT}$. Primer sequences are listed in Supplemental Table 1.

Table 1. Differentially upregulated gut metabolites in azoxymethane/dextran sulfate sodium-induced mice treated with lactoferrin hydrolysate (LFH).

Metabolite	VIP value	Abundance of Model group	Abundance of LFH group	*p* value
Chrysogine	4.4157	3.91 ± 0.16	5.07 ± 0.52	< 0.05
5'-Deoxy-5-Fluorocytidine	3.8605	3.17 ± 0.50	4.31± 0.72	< 0.05
Agmatine	3.7171	3.19 ± 0.41	4.34 ± 0.88	< 0.05
4-[[1-(3-Chloro-4-Fluorobenzoyl)Piperidin-3-Yl]Methoxy]-N-Propan-2-Ylbenzamide	2.9275	4.98 ± 0.38	5.67 ± 0.41	< 0.05
Glutamyl-Gamma-Glutamate	2.7752	4.77 ± 0.55	5.43 ± 0.19	< 0.05
(2S,3S)-1-[[2-Methoxy-5-(Trifluoromethoxy)Phenyl]Methyl]-2-Phenylpiperidin-3-Amine	2.6206	5.31 ± 0.33	5.88 ± 0.34	< 0.05
Methylphenidate	2.527	4.52 ± 0.18	4.93 ± 0.11	< 0.05
4-[5-(Benzenesulfonamido)-1-Methylbenzimidazol-2-Yl]-N,N-Diethylbenzamide	2.5056	5.70 ± 0.32	6.24 ± 0.33	< 0.05
Diferuloyl Putrescine	2.2934	6.52 ± 0.23	6.97 ±0.31	< 0.05
N-Cyclopentyl-1-(4-Ethoxyphenyl)Sulfonylpiperidine-4-Carboxamide	2.2092	4.48 ± 0.15	4.93 ± 0.41	< 0.05

2.8 Immunofluorescence analysis

After dewaxing, sections underwent antigen retrieval with EDTA buffer. Samples were blocked with 3% BSA for 30 min and incubated overnight at 4℃ with primary antibodies against Cyclin D1 (1:1000) or β-catenin (1:600). After washing, sections were incubated for 1 h at 25℃ with the corresponding Cy3-labeled secondary antibodies (1:300). Nuclei were counterstained with DAPI, autofluorescence was quenched, and slides were mounted. Fluorescent images were captured using a Nikon Eclipse C1 microscope (Nikon Corporation, Tokyo, Japan), and fluorescence intensity was quantified using Image-Pro Plus 6.0 (Media Cybernetics, Bethesda, MD, USA).

2.9 16S rRNA gene sequencing analysis

Total DNA was extracted from fecal samples. The V3–V4 region of the 16S rRNA gene was amplified using primers 338F (5′-ACTCCTACGGGAGGCAGCAG-3′) and 806R (5′-GGACTACHVGGGTWTCTAAT-3′). Sequencing was performed on an Illumina HiSeq 4000 platform (Illumina, San Diego, CA, USA). Raw reads were quality-filtered, merged based on overlapping regions, and denoised to obtain ASV representative sequences and abundance tables. Subsequent analyses and visualization were conducted using the Majorbio Cloud Platform (https://cloud.majorbio.com).

2.10 Non-targeted metabolomics analysis of gut metabolites

Fecal samples (50 ± 5 mg) were mixed with grinding beads and extracted with 400 μL of methanol-water (4:1, v/v). The mixtures were homogenized for 6 min at -10℃ (50 Hz), sonicated for 30 min at 5℃ (40 kHz), incubated at -20℃ for 30 min, and then centrifuged at 13,000 × g for 15 min at 4℃. The supernatant was evaporated under nitrogen, reconstituted in acetonitrile-water (1:1, v/v), ultrasonicated for 5 min, and

centrifuged again at 13,000 × g for 5 min. The final supernatant was transferred to LC-MS vials for subsequent analysis.

Chromatographic separation was performed on an ACQUITY UPLC HSS T3 column (100 mm × 2.1 mm, 1.8 μm). Mobile phase A consisted of 95% water and 5% acetonitrile (0.1% formic acid), and mobile phase B consisted of 47.5% acetonitrile, 47.5% isopropanol, and 5% water (0.1% formic acid). The injection volume was 3 μL, and the column temperature was 40℃. Data processing was conducted using Progenesis QI (Waters Corporation, Milford, USA). Mass detection, peak alignment, and metabolite identification were performed by matching MS and MS/MS spectra to metabolomics databases with a mass error threshold <10 ppm. Identified metabolites were used for further statistical and pathway analyses.

2.11 Statistical analysis

Normality was assessed using the Shapiro-Wilk test, and homogeneity of variance using Levene's test. One-way ANOVA followed by Tukey's post-hoc test was performed using GraphPad Prism 8 (GraphPad Software, San Diego, CA, USA). Data are presented as mean ± standard deviation. A p-value <0.05 was considered statistically significant.

3. Results

3.1 LFH alleviates AOM/DSS-induced colon cancer in mice

Body weight and colon length are important quantitative indicators for evaluating the progression of colon cancer. As shown in Figure 1A, mice in the AOM/DSS group exhibited significantly lower body weight compared with the control group at the end of the experiment ($P < 0.05$). LFH treatment did not significantly affect body weight relative to the AOM/DSS group ($P > 0.05$). Similarly, colon length was markedly reduced in the AOM/DSS group compared with the control group (Figure 1B; $P < 0.05$), whereas LFH administration did not produce a significant recovery in colon length ($P > 0.05$).

To further assess the therapeutic potential of LFH, histopathological changes and serum pro-inflammatory cytokines were examined. As shown in Figure 1C, colonic tissues from the control group displayed intact and well-organized crypt structures, abundant goblet cells, and preserved mucosal and muscular layers. In contrast, AOM/DSS-treated mice exhibited severe crypt loss, architectural distortion, goblet cell depletion, and prominent inflammatory cell infiltration. LFH treatment partially restored colonic structure, evidenced by more intact crypt architecture, increased goblet cell numbers, and reduced inflammatory infiltration compared with the AOM/DSS group. Consistent with these findings, serum levels of IL-1β, IL-6, and TNF-α were significantly elevated in AOM/DSS-treated mice by 1.38-, 1.48-, and 2.50-fold, respectively, compared with the control group (Figures 1D–F; $P < 0.05$). LFH administration significantly reduced these cytokine levels by 1.28-, 1.44-, and 2.24-fold, respectively ($P < 0.05$). The serum tumor markers CEA and CA19-9 also increased significantly in the AOM/DSS group—by 1.67- and 1.32-fold, respectively—relative to the control group (Figures 2A, B; $P < 0.05$). LFH treatment markedly decreased CEA and CA19-9 levels by 1.66- and 1.29-fold compared with the AOM/DSS group ($P < 0.05$). Ki-67, a

nuclear antigen associated with cell proliferation and tumor aggressiveness, was significantly elevated in AOM/DSS-treated mice, showing a 3.18-fold increase relative to controls (Figures 2D, E; $P < 0.05$). LFH treatment significantly reduced the number of Ki-67-positive cells by 1.94-fold ($P < 0.05$).

Together, these results demonstrate that LFH mitigates AOM/DSS-induced colon cancer by improving colonic histopathology, reducing systemic inflammation, and suppressing abnormal cellular proliferation.

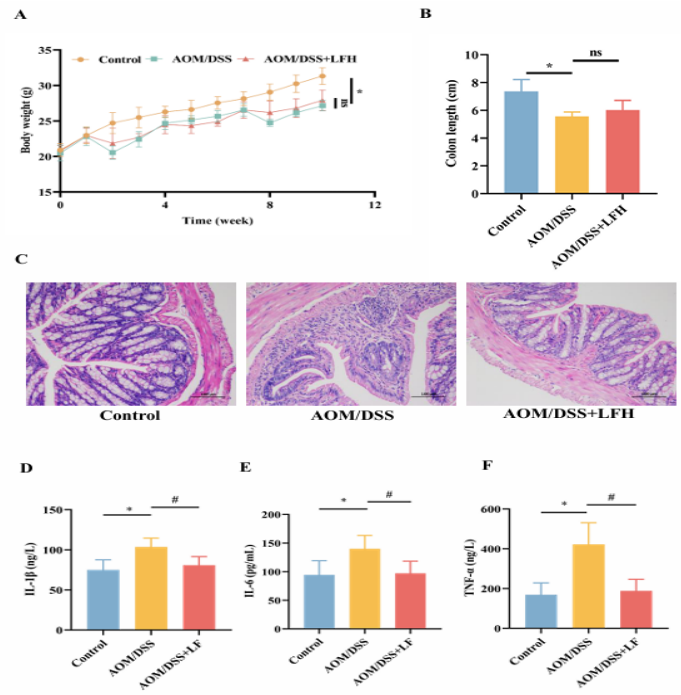

Figure 1. Effects of lactoferrin hydrolysate (LFH) on body weight, colon index, and serum pro-inflammatory cytokines in azoxymethane/dextran sulfate sodium (AOM/DSS)-treated mice. (A) Weekly body-weight changes; (B) colon length; (C) histopathological staining of colonic tissues; (D) serum interleukin (IL)-1β levels; (E) serum IL-6 levels; (F) serum tumor necrosis factor (TNF)-α levels. * indicates $P < 0.05$ compared with the control group; # indicates $P < 0.05$ compared with the model group; ns indicates no significant difference.

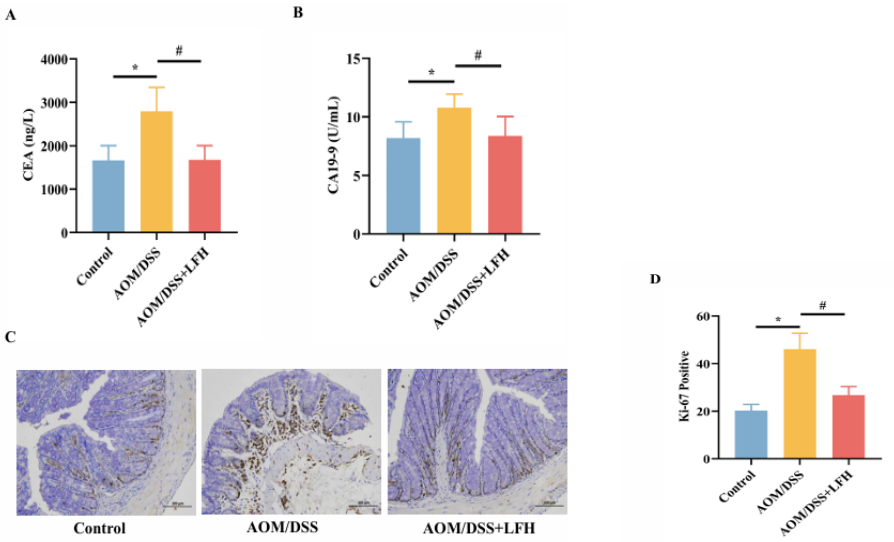

Figure 2. Effects of lactoferrin hydrolysate (LFH) on tumor markers and cell proliferation in azoxymethane/dextran sulfate sodium (AOM/DSS)-treated mice. (A) Serum carcinoembryonic antigen (CEA) levels; (B) serum carbohydrate antigen (CA) 19-9 levels; (C) Ki-67 immunohistochemistry of colonic tissues; (D) quantification of Ki-67-positive cells. * indicates $P < 0.05$ compared with the control group; # indicates $P < 0.05$ compared with the model group.

3.2 LFH inhibits activation of the Wnt/β-catenin signaling pathway

To evaluate whether LFH modulates the Wnt/β-catenin signaling pathway, the expression of key pathway-related genes was measured in colonic tissues. As shown in Figures 3A-C, AOM/DSS induction resulted in a significant upregulation of cellular myelocytomatosis oncogene (c-Myc), β-catenin, and Cyclin D1 compared with the control group ($P < 0.05$). LFH treatment markedly reduced the expression of these genes by 2.07-, 3.17-, and 2.56-fold, respectively ($P < 0.05$).

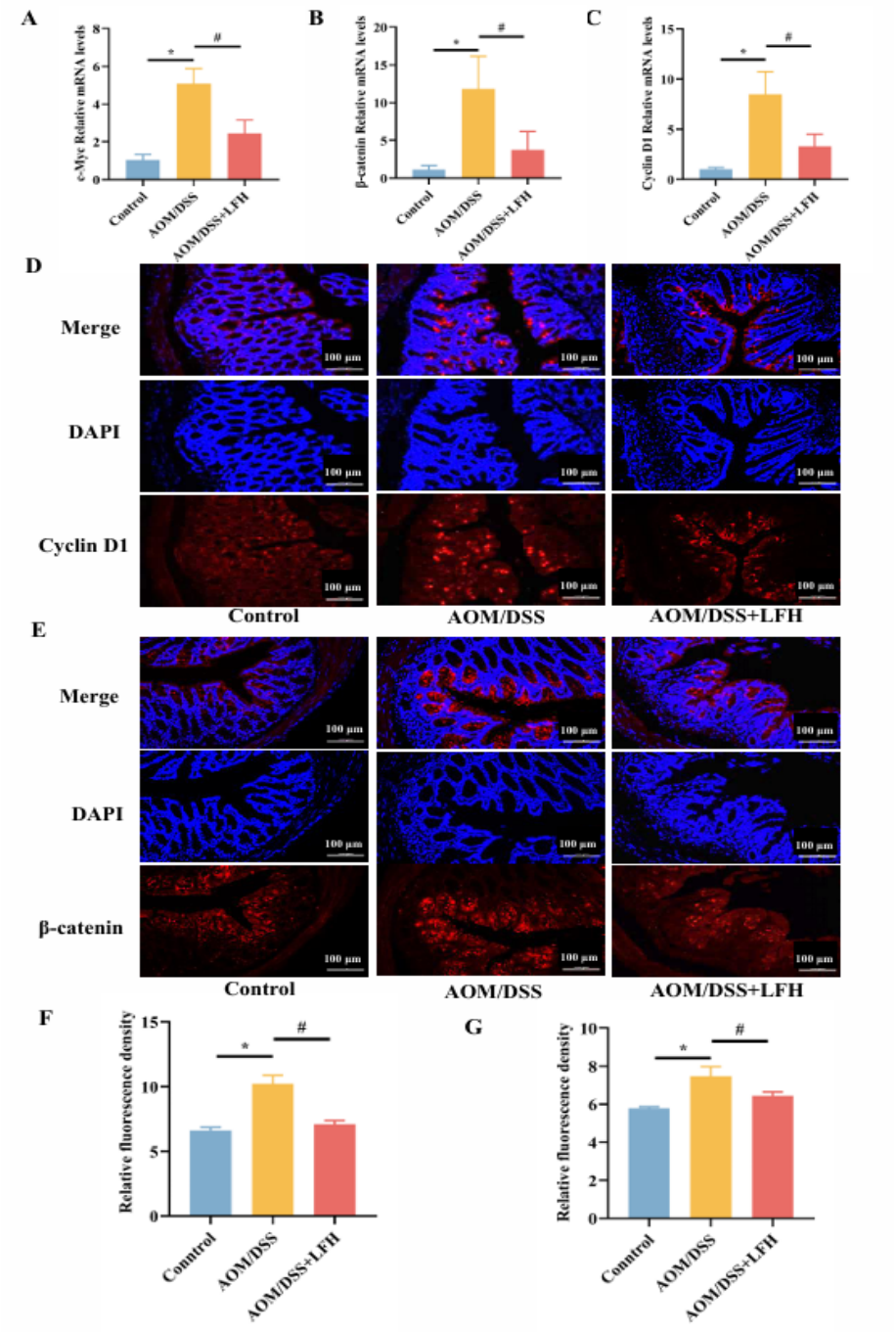

Figure 3. Effects of lactoferrin hydrolysate (LFH) on the wingless/integration site β-catenin (Wnt/β-catenin) signaling pathway in azoxymethane/dextran sulfate sodium (AOM/DSS)-treated mice. (A) Relative expression of cellular myelocytomatosis oncogene (c-Myc); (B) relative expression of β-catenin; (C) relative expression of Cyclin D1; (D) immunofluorescence staining of Cyclin D1; (E) immunofluorescence staining of β-catenin; (F) relative fluorescence intensity of Cyclin D1; (G) relative fluorescence intensity of β-catenin. * indicates $P < 0.05$ compared with the control group; # indicates $P < 0.05$ compared with the model group.

Protein expression was assessed by immunofluorescence. As illustrated in Figures 3D–G, β-catenin and Cyclin D1 protein levels were significantly elevated in the AOM/DSS group relative to the control group ($P < 0.05$). LFH administration significantly decreased the fluorescence intensity of both proteins ($P < 0.05$), consistent with the qRT-PCR results. These findings indicate that LFH alleviates AOM/DSS-induced colon cancer, at least in part, by suppressing the Wnt/β-catenin signaling pathway.

3.3 LFH regulates apoptosis-related genes in colonic tumor tissues

To determine whether LFH influences apoptosis in tumor tissues, the mRNA expression of key apoptosis-related genes was assessed in the colons of mice. As shown in Figure 4, AOM/DSS induction markedly decreased the expression of the pro-apoptotic genes Bcl-2-associated X protein (Bax), caspase-9, caspase-3, and p53 compared with the control group ($P < 0.05$). LFH administration significantly restored the expression of all four genes ($P < 0.05$). Conversely, the expression of the anti-apoptotic genes Bcl-2 and B-cell lymphoma-extra large (Bcl-xl) was significantly elevated following AOM/DSS induction ($P < 0.05$). LFH treatment reversed this trend, leading to a significant reduction in Bcl-2 and Bcl-xl expression ($P < 0.05$). These findings indicate that AOM/DSS disrupts the normal apoptotic regulatory network, enabling tumor cells to evade apoptosis and proliferate. LFH counteracts this dysregulation by modulating apoptosis-related gene expression, thereby promoting apoptotic activity in colonic tumor tissues.

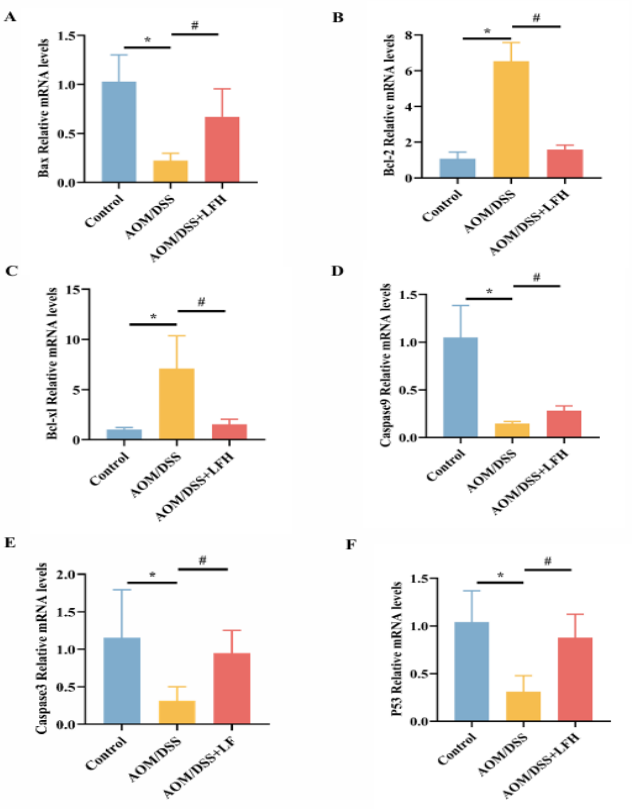

Figure 4. Effects of lactoferrin hydrolysate (LFH) on apoptosis-related gene expression in azoxymethane/dextran sulfate sodium (AOM/DSS)-treated mice. (A) Relative expression of Bcl-2-associated X protein (Bax); (B) relative expression of B-cell lymphoma 2 (Bcl-2); (C) relative expression of B-cell lymphoma-extra large (Bcl-xl); (D) relative expression of cysteine-aspartic acid protease (caspase)-9; (E) relative expression of caspase-3; (F) relative expression of tumor protein p53 (p53). * indicates $P < 0.05$ compared with the control group; # indicates $P < 0.05$ compared with the model group.

3.4 Effects of LFH on the gut microbiota of AOM/DSS-induced colon cancer mice

To evaluate the impact of LFH on gut microbiota in AOM/DSS-induced colon cancer mice, both α-diversity and β-diversity analyses were performed. As shown in Figures 5A–D, α-diversity indices (Ace, Chao, and Shannon) were significantly reduced in the AOM/DSS group relative to the control group ($P < 0.05$), indicating a marked decline in microbial richness and diversity. LFH treatment significantly restored these indices ($P < 0.05$). For the Simpson index, AOM/DSS induction resulted in a slight but nonsignificant decrease ($P > 0.05$), and LFH administration led to a nonsignificant upward trend ($P > 0.05$). As shown in Figure 5E, β-diversity analysis revealed clear separation between the Control and AOM/DSS groups, indicating substantial structural shifts in microbial communities. LFH treatment partially shifted the microbial profile away from the AOM/DSS group, demonstrating distinct clustering among the three groups.

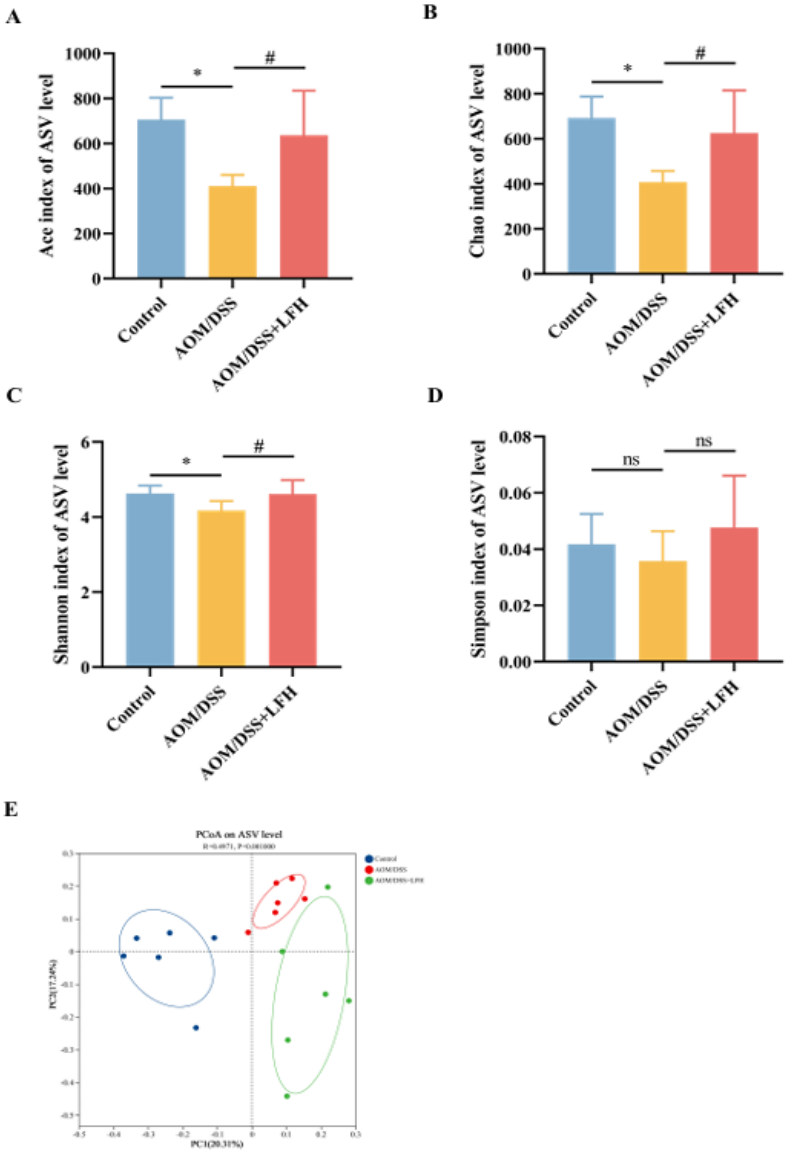

Figure 5. Effects of lactoferrin hydrolysate (LFH) on gut microbiota diversity in azoxymethane/dextran sulfate sodium (AOM/DSS)-treated mice. (A) Ace index; (B) Chao index; (C) Shannon index; (D) Simpson index; (E) Principal coordinates analysis (PCoA) plot of gut microbiota. * indicates $P < 0.05$ compared with the control group; # indicates $P < 0.05$ compared with the model group; ns indicates no significant difference.

At the phylum level (Figure 6A), *Firmicutes* and *Bacteroidota* were the dominant taxa in all groups. The *Firmicutes*/*Bacteroidota* ratios in the Control, AOM/DSS, and AOM/DSS+LFH groups were 1.28 ± 0.45, 1.68 ± 0.67, and 1.30 ± 0.70, respectively, with significant differences among groups ($P < 0.05$; Figure 6B). At the genus level (Figures 6C and 6D), AOM/DSS induction significantly increased the abundance of *Bacillus*, *Turicibacter*, *Enterorhabdus*, *Odoribacter*, *Clostridium_sensu_stricto_1*, and *Romboutsia* ($P < 0.05$), while significantly reducing *Ruminococcus*, *Akkermansia*, *Allobaculum*, and *Eubacterium_siraeum_group* ($P < 0.05$). LFH treatment reduced the abundance of *Bacillus*, *Enterorhabdus*, *Odoribacter*, and *Romboutsia*, while increasing the abundance of *Ruminococcus*, *Akkermansia*, and *Eubacterium_siraeum_group*. Linear discriminant analysis effect size (LEfSe) analysis (Figure 6F) further showed that *Ruminococcus*, *Akkermansiaceae*, *Eubacterium_siraeum_group*, and *Allobaculum* were enriched in the control group, whereas *Bacillus*, *Odoribacter*, and *Enterorhabdus* were enriched in the AOM/DSS group. *Turicibacter* and *Clostridium_sensu_stricto_1* were characteristic taxa in the AOM/DSS + LFH group.

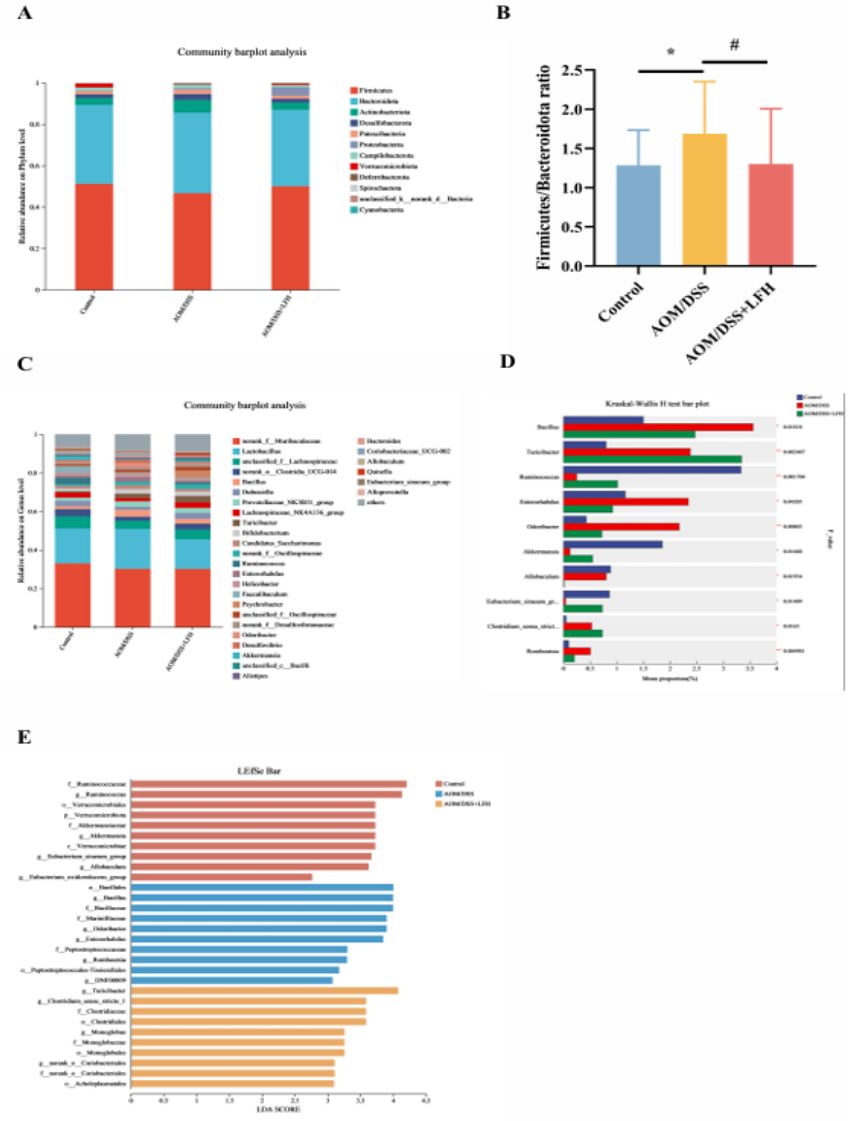

Figure 6. Effects of lactoferrin hydrolysate (LFH) on gut microbiota composition at the phylum and genus levels in azoxymethane/dextran sulfate sodium (AOM/DSS)-treated mice. (A) Relative abundance at the phylum level; (B) *Firmicutes*/*Bacteroidota* ratio, * indicates $P < 0.05$ compared with the control group; # indicates $P < 0.05$ compared with the model group; (C) relative abundance at the genus level; (D) significantly different genera, * $P < 0.05$, ** $P < 0.01$; (E) Linear discriminant analysis (LDA) discriminant bar chart.

To explore associations between gut microbiota and disease-related indicators, the top 30 genera were correlated with physiological parameters, serological markers, and gene-expression profiles (Figure 7). Notably, TNF-α, IL-6, and IL-1β were positively correlated with *Bacillus* and *Odoribacter*, and negatively correlated with *Ruminococcus*. Tumor markers CEA and CA19-9 showed positive correlations with *Enterorhabdus*, but negative correlations with *Ruminococcus*, *Eubacterium_siraeum_group*, and *Lachnospiraceae_NK4A136_group*. Key oncogenic genes (c-Myc, Cyclin D1, and β-catenin) showed a positive correlation with *Odoribacter* and a negative correlation with *Ruminococcus*. The anti-apoptotic genes (Bcl-2 and Bcl-xl) were positively correlated with *Enterorhabdus* and *Prevotellaceae_NK3B31_group*, and negatively correlated with *Ruminococcus*. The pro-apoptotic genes (Bax and p53) exhibited positive correlations with *Ruminococcus*, but negative correlations with *Bacillus*, *Odoribacter*, and *Enterorhabdus*. Among the taxa analyzed, *Bacillus*, *Odoribacter*, *Enterorhabdus*, *Ruminococcus*, *Eubacterium_siraeum_group*, and *Lachnospiraceae_NK4A136_group* each showed significant correlations with five or more colon-cancer-related indicators. Taken together, these findings suggest that *Bacillus*, *Enterorhabdus*, and *Odoribacter*—substantially enriched after AOM/DSS induction and strongly associated with adverse physiological indicators—may function as harmful bacteria contributing to tumor progression. In contrast, *Ruminococcus* and *Eubacterium_siraeum_group*, which were markedly reduced by AOM/DSS but restored after LFH treatment, and which correlated negatively with inflammation and tumor markers, may serve as beneficial taxa mediating the protective effects of LFH on colon cancer.

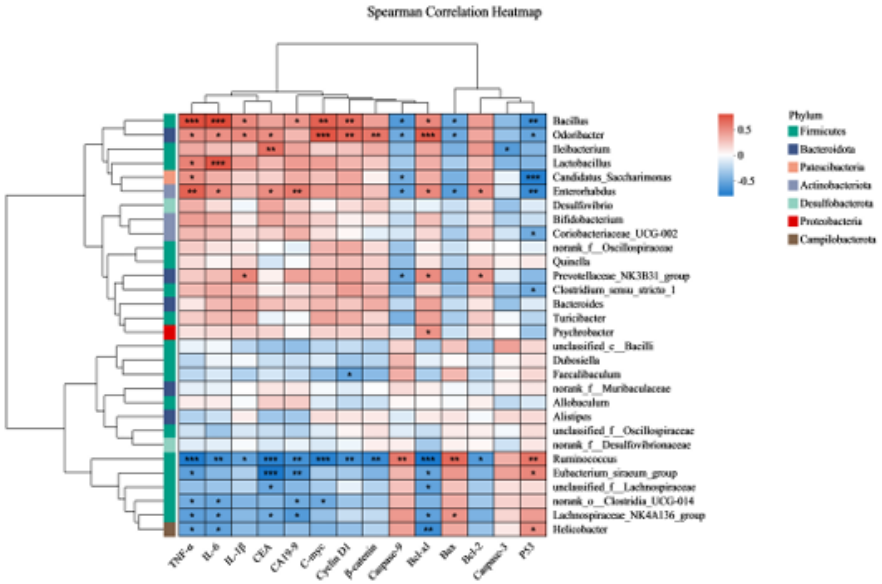

Figure 7. Correlation analysis of relative gut microbial abundance with colon cancer-related parameters. * $P < 0.05$, ** $P < 0.01$, *** $P < 0.001$.

3.5 The effect of LFH on gut metabolites in mice with colon cancer

To evaluate metabolic alterations associated with LFH treatment, multivariate statistical analyses were performed on fecal metabolites. As shown in Figure 8A, partial least squares discriminant analysis (PLS-DA)

revealed a clear separation between the Control and AOM/DSS groups, indicating substantial metabolic disturbances induced by AOM/DSS. Following LFH administration, the AOM/DSS+LFH group also separated distinctly from the AOM/DSS group, suggesting that LFH exerted a marked regulatory effect on gut metabolism. The validity of the PLS-DA model was confirmed by permutation testing (Figure 8B), in which the Q^2 regression line intercepted below 0.05 on the Y-axis, demonstrating the absence of model overfitting.

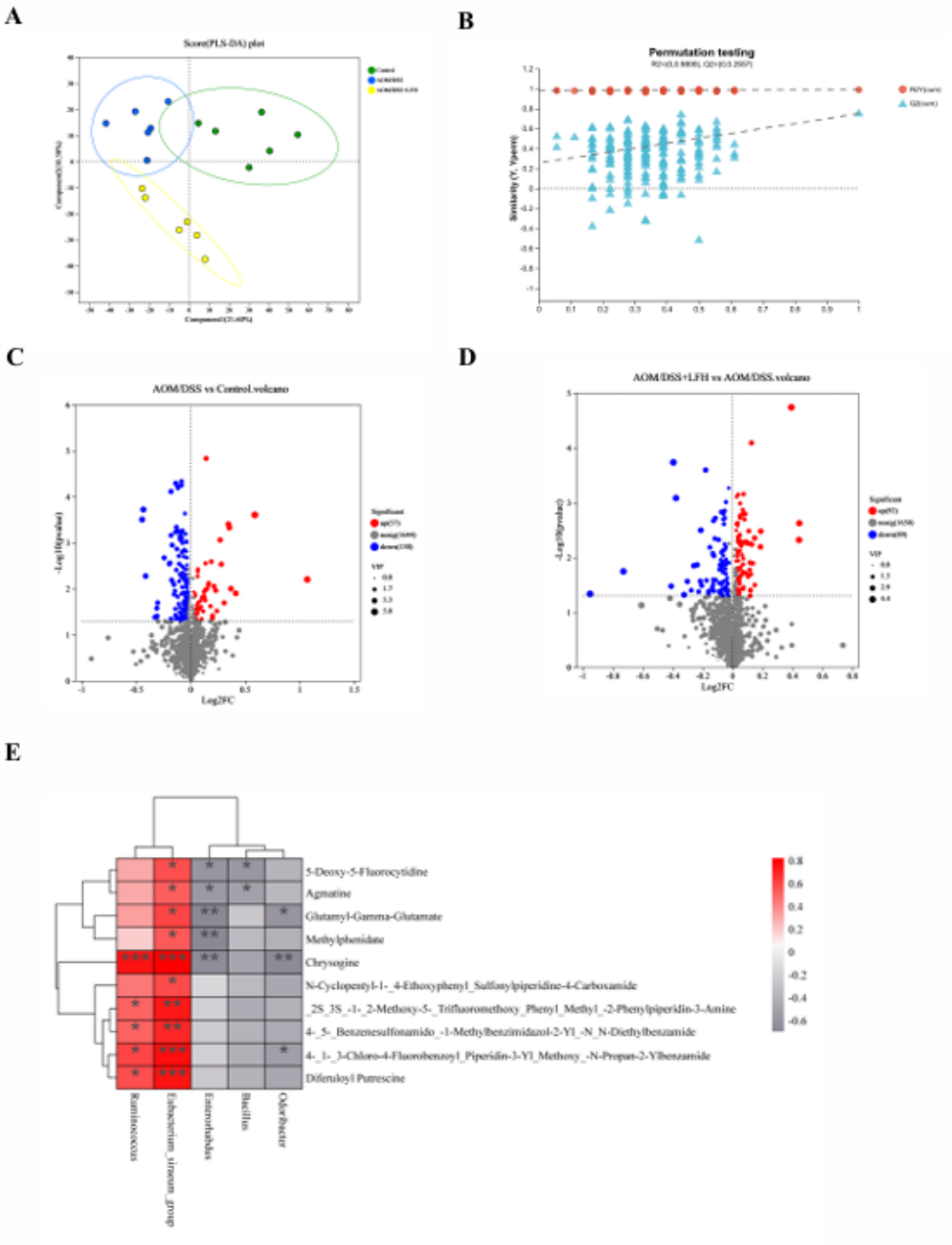

Figure 8. Effects of lactoferrin hydrolysate (LFH) on gut metabolites in azoxymethane/dextran sulfate sodium (AOM/DSS)-treated mice. (A) Partial least squares-discriminant analysis (PLS-DA) score plot; (B) PLS-DA permutation test; (C) volcano plot of differential metabolites (Model vs Control); (D) volcano plot of differential metabolites (LFH vs Model); (E) correlation analysis between gut microbiota and differential metabolites. * $P < 0.05$, ** $P < 0.01$, *** $P < 0.001$.

Volcano plot analysis (Figures 8C and 8D) identified differential metabolites between groups. Relative to the control group, the AOM/DSS group exhibited 57 significantly upregulated and 130 significantly downregulated metabolites. Compared with the AOM/DSS group, LFH treatment resulted in 92 significantly upregulated and 89 significantly downregulated metabolites. Based on the criteria of VIP > 1 and $P < 0.05$, the ten most strongly upregulated metabolites in the AOM/DSS+LFH group were identified (Table 1), including Chrysogine, 5′-Deoxy-5-Fluorocytidine, Agmatine, Glutamyl-Gamma-Glutamate, and several additional small-molecule compounds.

To further identify microbiota-associated metabolites influenced by LFH, correlations between the ten most upregulated metabolites and five key bacterial genera were analyzed (Figure 8E). Several metabolites—such as (2S,3S)-1-[[2-Methoxy-5-(Trifluoromethoxy) Phenyl] Methyl]-2-Phenylpiperidin-3-Amine, 4-[5-(Benzenesulfonamido)-1-Methylbenzimidazol-2-yl]-N,N-Diethylbenzamide, Diferuloyl Putrescine, and 4-[[1-(3-Chloro-4-Fluorobenzoyl)Piperidin-3-yl]Methoxy]-N-Propan-2-ylbenzamide—showed significant positive correlations with *Ruminococcus* and *Eubacterium_siraeum_group*. Chrysogine was also positively correlated with these two taxa, while 5'-Deoxy-5-Fluorocytidine, Agmatine, Glutamyl-Gamma-Glutamate, Methylphenidate, and N-Cyclopentyl-1-(4-Ethoxyphenyl)Sulfonylpiperidine-4-Carboxamide were positively correlated with *Eubacterium_siraeum_group* alone. In contrast, several metabolites displayed significant negative correlations with harmful taxa. For example, 5′-Deoxy-5-Fluorocytidine and Agmatine were negatively correlated with *Enterorhabdus* and *Bacillus*. Glutamyl-Gamma-Glutamate and Chrysogine showed negative correlations with *Odoribacter* and *Enterorhabdus*, while Methylphenidate and 4-[[1-(3-Chloro-4-Fluorobenzoyl)Piperidin-3-yl]Methoxy]-N-Propan-2-ylbenzamide were negatively correlated with *Enterorhabdus* and *Odoribacter*, respectively. Overall, five metabolites—Chrysogine, Agmatine, 5′-Deoxy-5-Fluorocytidine, Glutamyl-Gamma-Glutamate, and 4-[[1-(3-Chloro-4-Fluorobenzoyl)Piperidin-3-yl]Methoxy]-N-Propan-2-ylbenzamide—showed significant correlations with at least three bacterial genera, suggesting that they may represent key microbial metabolites associated with the beneficial effects of LFH.

4. Discussion

In the AOM/DSS-induced mouse model of colon cancer, chronic inflammation and tumorigenesis jointly exert profound effects on colonic structure and function. A key pathological feature is the disruption of crypt architecture, which compromises intestinal homeostasis and promotes adenoma formation and progression [18]. Consistent with previous reports, the AOM/DSS group in this study displayed substantial crypt loss, architectural distortion, reduced goblet cells, and marked inflammatory infiltration. LFH administration mitigated these histopathological alterations, as evidenced by improved crypt integrity, increased goblet cell numbers, and reduced inflammatory cell infiltration, suggesting that LFH can attenuate AOM/DSS-induced colonic injury. Pro-inflammatory cytokines such as IL-1β, IL-6, and TNF-α are major mediators of chronic inflammation and are closely associated with the development of inflammation-driven colorectal cancer [19]. Their elevated expression in AOM/DSS-induced models is recognized as a critical contributor to tumor progression, and reducing these cytokines can alleviate inflammatory responses and suppress disease

development [20]. In agreement with earlier findings, LFH treatment markedly decreased serum IL-1β, IL-6, and TNF-α levels, indicating a significant anti-inflammatory effect that may contribute to its protective role in colon cancer. Tumor markers play an important role in the early screening, auxiliary diagnosis, prognosis assessment, therapeutic evaluation, and recurrence monitoring of colon cancer [21]. Among them, CEA is one of the most widely applied clinical markers. An elevated serum CEA concentration is often closely associated with the presence, progression, and even recurrence of tumors, and is therefore commonly used for monitoring colon cancer [22]. CA19-9, a high-molecular-weight mucin-associated polysaccharide antigen, is also widely expressed in gastrointestinal tumors and serves as an important indicator in their clinical evaluation [23]. Previous studies showed that AOM/DSS induction elevates serum CEA and CA19-9, while therapeutic interventions can reduce their levels [24-26]. Similarly, LFH significantly lowered both CEA and CA19-9 compared with the AOM/DSS group, further supporting its role in attenuating tumor development. The dysregulation of cell-cycle control is one of the core molecular mechanisms underlying the initiation and progression of malignant tumors. It is characterized by sustained activation of proliferative signaling pathways and impaired cell-cycle checkpoints [27]. Compared with normal cells, tumor cells exhibit uncontrolled proliferative behavior, and various molecular markers are used to detect and evaluate this abnormal proliferative state [28]. Ki-67 is a nuclear antigen associated with cell proliferation and is aberrantly expressed in numerous tumors and precancerous lesions. Its expression level reflects the proliferative activity of tumor cells and is closely associated with tumor initiation, progression, metastatic potential, and treatment response. An elevated Ki-67 index indicates enhanced proliferative capacity of colon cancer cells, thereby contributing to cancer progression [29, 30]. Previous studies have shown that Ki-67 expression is significantly reduced after therapeutic intervention in colon cancer models [30], and inhibiting Ki-67 expression has been reported to exert antitumor effects [31]. Consistent with these findings, LFH administration markedly reduced the number of Ki-67–positive cells in AOM/DSS-induced mice compared with the model group, suggesting that LFH effectively suppresses malignant proliferation in tumor tissues. In summary, LFH alleviates AOM/DSS-induced colon cancer by mitigating pathological damage, reducing the pro-inflammatory cytokines IL-1β, IL-6, and TNF-α, lowering the serum tumor markers CEA and CA19-9, and suppressing aberrant cellular proliferation—as evidenced by decreased Ki-67 expression.

The Wnt signaling pathway is a complex and highly conserved regulatory system throughout biological evolution. Among its branches, the Wnt/β-catenin signaling cascade plays a crucial role in maintaining cellular homeostasis and is also widely implicated in the initiation and progression of various cancers [32, 33]. Under cancerous conditions, the β-catenin–regulated Wnt pathway becomes aberrantly activated, leading to impaired phosphorylation and degradation of β-catenin. Consequently, β-catenin accumulates in the cytoplasm, translocates into the nucleus, and binds to transcription factors of the TCF/LEF family, thereby promoting the transcription of downstream oncogenic targets such as c-Myc and Cyclin D1. These events collectively regulate cell proliferation, differentiation, migration, and apoptosis [34, 35]. In the present study, AOM/DSS induction markedly upregulated key genes and downstream effectors of this pathway, including c-Myc, β-

catenin, and Cyclin D1. LFH treatment significantly reduced their expression, suggesting that LFH may exert protective effects against AOM/DSS-induced colon cancer by suppressing aberrant activation of the Wnt/β-catenin axis.

Cell apoptosis is an essential physiological process that removes abnormal or damaged cells, thereby preventing tumor development [36]. Growing evidence indicates that promoting apoptosis represents a major anticancer strategy for numerous therapeutic compounds [37, 38]. Apoptosis involves both intrinsic and extrinsic pathways, among which the intrinsic mitochondrial pathway plays a central role in suppressing colon cancer progression [39]. This pathway is primarily regulated by the p53/caspase axis and the Bcl-2 protein family. As a key tumor suppressor, p53 initiates apoptosis by activating transcription of pro-apoptotic genes such as Bax while repressing anti-apoptotic genes including Bcl-2 [40], and also triggers the downstream caspase cascade [41]. In colon cancer, impairment of p53 function frequently contributes to apoptotic escape [42]. Within the mitochondrial pathway, the balance between pro-apoptotic Bax and anti-apoptotic Bcl-2 and Bcl-xl determines whether cells undergo apoptosis [43, 44]. Bax facilitates mitochondrial membrane permeabilization and release of apoptogenic factors [45], whereas Bcl-2 and Bcl-xl counteract apoptosis by inhibiting Bax activity [46]. An increase in Bax accompanied by a decrease in Bcl-2/Bcl-xl is widely recognized as a hallmark of intrinsic apoptotic pathway activation [47].Caspase-9 acts as the initiator caspase of the intrinsic apoptotic pathway [48]. It can be activated either through p53-mediated signaling or by cytochrome c released from mitochondria [49, 50]. Activated caspase-9 subsequently triggers the downstream executioner caspase-3 [48, 49], which cleaves multiple intracellular substrates to complete the programmed cell death process [48, 51]. Accordingly, evaluating the expression of these apoptosis-related genes provides meaningful insight into intrinsic apoptotic pathway activation. Previous research has shown that upregulation of Bax accompanied by downregulation of Bcl-2 and Bcl-xl activates the mitochondrial apoptotic pathway, leading to caspase-9 activation and subsequent caspase-3-mediated execution of apoptosis [52]. Consistent with previous findings, LFH treatment significantly increased Bax expression while decreasing Bcl-2 and Bcl-xl levels in AOM/DSS-induced colon cancer mice, suggesting reduced apoptotic resistance in tumor cells. Furthermore, LFH enhanced the expression of p53, caspase-9, and caspase-3, providing additional evidence that LFH promotes activation of the intrinsic apoptotic pathway in colonic tissues.

The human gastrointestinal tract contains a complex and diverse microbial community that plays a central role in host health and gut immune regulation. Disruption of gut microbial homeostasis can alter the intestinal microenvironment and contribute to gastrointestinal diseases, including colon cancer [16]. Increasing evidence suggests that gut microbiota dysbiosis facilitates colon cancer progression, whereas specific dietary components may alleviate colon cancer by modulating microbial composition [8, 53]. In this study, LFH treatment markedly increased Ace, Chao, and Shannon diversity indices. β-diversity analysis further demonstrated significant differences among groups, indicating that LFH effectively reshaped the gut microbial structure disrupted by AOM/DSS induction. This finding aligns with previous reports showing that quinoa peptides improved gut microbial profiles in colon cancer models [8]. At the phylum level, changes in the

Firmicutes/*Bacteroidetes* ratio are closely linked to intestinal inflammation and inflammation-associated colorectal cancer, while restoring this ratio may help suppress colorectal tumorigenesis [54]. Similar to findings with *Sparassis latifolia*, which lowered this ratio and alleviated colon cancer symptoms [16], LFH reduced the elevated *Firmicutes*/*Bacteroidetes* ratio observed in AOM/DSS mice, implying that modulating microbial balance may contribute to its protective effects. Further analysis at the genus level revealed notable shifts. *Bacillus* has been reported to secrete toxins that facilitate carcinogenic processes [55]; *Enterorhabdus* is associated with tumor growth [56]; and *Odoribacter* is a key taxon linked to colorectal adenoma/carcinoma microbiota [57]. In contrast, *Ruminococcus* is involved in short-chain fatty acid production [58], which suppresses inflammatory cytokine expression and promotes mucosal repair through inhibition of NF-κB pathway activation [59]. The *Eubacterium_siraeum_group* is recognized as a beneficial genus with protective roles in DSS-induced colitis [60]. Consistent with these findings, AOM/DSS induction in the present study significantly increased *Bacillus*, *Enterorhabdus*, and *Odoribacter* abundance, while decreasing *Ruminococcus* and *Eubacterium_siraeum_group*. LFH treatment partially restored these beneficial taxa to levels comparable to the control group. Importantly, *Bacillus*, *Odoribacter*, *Enterorhabdus*, *Ruminococcus*, and *Eubacterium_siraeum_group* were significantly correlated with at least five colon cancer–related physiological indicators, highlighting their functional relevance. These observations suggest that *Bacillus*, *Enterorhabdus*, and *Odoribacter* may serve as harmful bacteria contributing to AOM/DSS-induced colon cancer, whereas *Ruminococcus* and *Eubacterium_siraeum_group* may exert protective roles associated with LFH treatment. Microbial alterations were accompanied by marked shifts in gut metabolites. Metabolomic analysis allows identification of compounds associated with specific physiological or pathological states, advancing understanding of disease mechanisms. Chrysogine has been reported to disrupt tumor cell energy metabolism with potential antitumor activity [61, 62]. 5′-Deoxy-5-Fluorocytidine is a prodrug converted into 5-fluorouracil, a well-established chemotherapeutic agent that inhibits thymidylate synthase, induces nucleotide imbalance, and causes DNA damage responses, thereby suppressing tumor cell growth [63]. Agmatine inhibits tumor cell proliferation by down-modulating growth-promoting signaling pathways and activating apoptosis-associated proteins [64]. Glutamyl-gamma-glutamate has been shown to inhibit tumor growth by activating TLR4-dependent immune pathways [65]. In this study, LFH significantly increased the abundance of Chrysogine, Agmatine, 5′-Deoxy-5-Fluorocytidine, and Glutamyl-Gamma-Glutamate, all of which exhibited strong correlations with key gut bacterial genera. These findings suggest that LFH may alleviate colon cancer through coordinated modulation of both gut microbiota and their metabolites. Future studies are warranted to validate the roles of these key bacteria and metabolites in LFH-mediated protection using targeted cellular and animal experiments.

5. Conclusions

This study systematically investigated the alleviating effects of LFH on colon cancer using an AOM/DSS-induced mouse model. The findings demonstrated that LFH improved the histopathological morphology of colonic tissue, significantly reduced serum inflammatory cytokine levels, and inhibited the

abnormal cell proliferation induced by AOM/DSS, thereby exerting a notable protective effect against colon cancer. These beneficial effects appeared to be associated with the modulation of the Wnt/β-catenin signaling pathway and the regulation of apoptosis-related gene expression, which together contributed to enhanced apoptotic responses in tumor tissues. Moreover, LFH markedly influenced key gut microbial taxa and their associated metabolites, and these alterations showed significant correlations with its anti-colon cancer effects. In summary, this work provides new insights into how LFH may alleviate colon cancer and supports its potential application in the development of functional foods.

Acknowledgements

We thank the funding by the Science and Technology Research Program of the Chongqing Municipal Education Commission (KJQN202300204; KJZD-K202400206).

Declaration of interests

The authors declare that they have no known competing financial interests or personal relationships that could have appeared to influence the work reported in this paper.

References

[1] S.W. Yoo, G. Oh, A.M. Safi, et al., Endoscopic non-ablative fractional laser therapy in an orthotopic colon tumour model, Scientific Reports. 8 (2018) 1673. 1673. https://doi.org/10.1038/s41598-018-19792-2.

[2] S. Piawah, A.P. Venook, Targeted therapy for colorectal cancer metastases: A review of current methods of molecularly targeted therapy and the use of tumor biomarkers in the treatment of metastatic colorectal cancer, Cancer. 125 (2019) 4139-4147. https://doi.org/10.1002/cncr.32163.

[3] Y. Zhang, T. Mu, X. Deng, et al., New Insights of Biological Functions of Natural Polyphenols in Inflammatory Intestinal Diseases, International Journal of Molecular Sciences. 24 (2023) 9581. 9581. https://doi.org/10.3390/ijms24119581.

[4] J. Chen, Y. Gao, Y. Zhang, et al., Research progress in the treatment of inflammatory bowel disease with natural polysaccharides and related structure-activity relationships, Food & Function. 15 (2024) 5680-5702. https://doi.org/10.1039/d3fo04919a.

[5] C. Wang, C. Cui, N. Li, et al., Antioxidant activity and protective effect of wheat germ peptides in an in vitro celiac disease model via Keap1/Nrf2 signaling pathway, Food Research International. 161 (2022) 111864. 111864. https://doi.org/10.1016/j.foodres.2022.111864.

[6] J. Xie, Z. Hong, J. Dai, et al., Isolation and identification of anti-colorectal cancer peptides from walnut proteins and associated in silico analysis, Journal of Functional Foods. 112 (2024) 105952. 105952. https://doi.org/10.1016/j.jff.2023.105952.

[7] C. Murali, P. Mudgil, C.Y. Gan, et al., Camel whey protein hydrolysates induced G2/M cellcycle arrest in human colorectal carcinoma, Scientific Reports. 11 (2021) 7062. 7062. https://doi.org/10.1038/s41598-021-86391-z.

[8] X. Fan, H. Guo, C. Teng, et al., Supplementation of quinoa peptides alleviates colorectal cancer and restores gut microbiota in AOM/DSS-treated mice, Food Chemistry. 408 (2023) 135196. 135196. https://doi.org/10.1016/j.foodchem.2022.135196.

[9] X. Fan, H. Guo, C. Teng, et al., Anti-Colon Cancer Activity of Novel Peptides Isolated from In Vitro Digestion of Quinoa Protein in Caco-2 Cells, Foods. 11 (2022) 194. 194. https://doi.org/10.3390/foods11020194.

[10] J. Zhang, S. Lai, Z. Cai, et al., Determination of bovine lactoferrin in dairy products by ultra-high performance liquid chromatography-tandem mass spectrometry based on tryptic signature peptides employing an isotope-labeled winged peptide as internal standard, Analytica Chimica Acta. 829 (2014) 33-39. https://doi.org/10.1016/j.aca.2014.04.025.

[11] R. Hong, A. Xie, C. Jiang, et al., A review of the biological activities of lactoferrin: mechanisms and potential applications, Food & Function. 15 (2024) 8182-8199. https://doi.org/10.1039/d4fo02083a.

[12] S. Peled, S. Freilich, H. Hanani, et al., Next-generation prebiotics: Maillard-conjugates of 2′-fucosyllactose and lactoferrin hydrolysates beneficially modulate gut microbiome composition and health promoting activity in a murine model, Food

Research International. 177 (2024) 113830. 113830. https://doi.org/10.1016/j.foodres.2023.113830.

[13] M. Narmuratova, D. Berillo, Z. Narmuratova, et al., Antihypertensive, Anti-Inflammatory, and Antiangiogenic In Silico Activity of Lactoferrin-Derived Peptides of Equine Milk Hydrolysate, Biomedicines. 12 (2024) 2715. 2715. https://doi.org/10.3390/biomedicines12122715.

[14] O. Oussaief, Z. Jrad, I. Adt, et al., Antioxidant, lipase and ACE-inhibitory properties of camel lactoferrin and its enzymatic hydrolysates, International Journal of Dairy Technology. 76 (2023) 126-137. https://doi.org/10.1111/1471-0307.12904.

[15] R. Fernandez Musoles, J.B. Salom, D. Martinez Maqueda, et al., Antihypertensive effects of lactoferrin hydrolyzates: Inhibition of angiotensin and endothelin-converting enzymes, Food Chemistry. 139 (2013) 994-1000. https://doi.org/10.1016/j.foodchem.2012.12.049.

[16] X. Wei, F. Cheng, J. Liu, et al., Sparassis latifolia polysaccharides inhibit colon cancer in mice by modulating gut microbiota and metabolism, International Journal of Biological Macromolecules. 232 (2023) 123299. 123299. https://doi.org/10.1016/j.ijbiomac.2023.123299.

[17] M. Liu, W. Xie, X. Wan, et al., Clostridium butyricum modulates gut microbiota and reduces colitis associated colon cancer in mice, International Immunopharmacology. 88 (2020) 106862. 106862. https://doi.org/10.1016/j.intimp.2020.106862.

[18] F. Ma, M. Sun, Y. Song, et al., Lactiplantibacillus plantarum-12 Alleviates Inflammation and Colon Cancer Symptoms in AOM/DSS-Treated Mice through Modulating the Intestinal Microbiome and Metabolome, Nutrients. 14 (2022) 1916. 1916. https://doi.org/10.3390/nu14091916.

[19] H. Zhao, L. Wu, G. Yan, et al., Inflammation and tumor progression: signaling pathways and targeted intervention, Signal Transduction and Targeted Therapy. 6 (2021) 263. 263. https://doi.org/10.1038/s41392-021-00658-5.

[20] F. Ma, Y. Song, M. Sun, et al., Exopolysaccharide Produced by Lactiplantibacillus plantarum-12 Alleviates Intestinal Inflammation and Colon Cancer Symptoms by Modulating the Gut Microbiome and Metabolites of C57BL/6 Mice Treated by Azoxymethane/Dextran Sulfate Sodium Salt, Foods. 10 (2021) 3060. 3060. https://doi.org/10.3390/foods10123060.

[21] W.M. Steinberg, R. Gelfand, K.K. Anderson, et al., Comparsion of the sensitivity and specificity of the CA19-9 and carcinoembryonic antigen assays in detecting cancer of the pancreas, Gastroenterology. 90 (1986) 343-349. https://doi.org/10.1016/0016-5085(86)90930-3.

[22] O. Margalit, R. Mamtani, Y. Yang, et al., Assessing the prognostic value of carcinoembryonic antigen levels in stage I and II colon cancer, European Journal of Cancer. 94 (2018) 1-5. https://doi.org/10.1016/j.ejca.2018.01.112.

[23] J. Stiksma, D.C. Grootendorst, P.W.G. van der Linden, CA 19-9 As a Marker in Addition to CEA to Monitor Colorectal Cancer, Clinical Colorectal Cancer. 13 (2014) 239-244. https://doi.org/10.1016/j.clcc.2014.09.004.

[24] A. Seetha, H. Devaraj, G. Sudhandiran, Effects of combined treatment with Indomethacin and Juglone on AOM/DSS induced colon carcinogenesis in Balb/c mice: Roles of inflammation and apoptosis, Life Sciences. 264 (2021) 118654. 118657. https://doi.org/10.1016/j.lfs.2020.118657.

[25] H. Lin, X. Ma, X. Yang, et al., Natural shikonin and acetyl-shikonin improve intestinal microbial and protein composition to alleviate colitis-associated colorectal cancer, International Immunopharmacology. 111 (2022) 109097. 109097. https://doi.org/10.1016/j.intimp.2022.109097.

[26] S. Agah, A.M. Alizadeh, M. Mosavi, et al., More Protection of Lactobacillus acidophilus Than Bifidobacterium bifidum Probiotics on Azoxymethane-Induced Mouse Colon Cancer, Probiotics and Antimicrobial Proteins. 11 (2019) 857-864. https://doi.org/10.1007/s12602-018-9425-8.

[27] J. Li, B.Z. Stanger, Cell Cycle Regulation Meets Tumor Immunosuppression, Trends in Immunology. 41 (2020) 859-863. https://doi.org/10.1016/j.it.2020.07.010.

[28] N.H. Kim, M.J. Xin, J.Y. Cha, et al., Antitumor and Immunomodulatory Effect of Gastrodia elata on Colon Cancer In Vitro and In Vivo, American Journal of Chinese Medicine. 45 (2017) 319-335. https://doi.org/10.1142/s0192415x17500203.

[29] M. Sobecki, K. Mrouj, J. Colinge, et al., Cell-Cycle Regulation Accounts for Variability in Ki-67 Expression Levels, Cancer Research. 77 (2017) 2722-2734. https://doi.org/10.1158/0008-5472.Can-16-0707.

[30] Y. Zhou, X. Ji, D. Wang, et al., Effect of silkworm pupae (Bombyx mori) protein on colon cancer in nude mice: inhibition of tumor growth, oxidative stress and inflammatory response, Frontiers in Pharmacology. 14 (2023) 1138742. 1138742. https://doi.org/10.3389/fphar.2023.1138742.

[31] L. Ma, G.B. Xu, X. Tang, et al., Anti-cancer potential of polysaccharide extracted from hawthorn (Crataegus.) on human colon cancer cell line HCT116 via cell cycle arrest and apoptosis, Journal of Functional Foods. 64 (2020) 103677. 103677. https://doi.org/10.1016/j.jff.2019.103677.

[32] H. Dou, R. Shen, J. Tao, et al., Curcumin Suppresses the Colon Cancer Proliferation by Inhibiting Wnt/β-Catenin Pathways via miR-130a, Frontiers in Pharmacology. 8 (2017) 00877. 877. https://doi.org/10.3389/fphar.2017.00877.

[33] R. Yan, H. Zhu, P. Huang, et al., Liquidambaric acid inhibits Wnt/β-catenin signaling and colon cancer via targeting TNF receptor-associated factor 2, Cell Reports. 38 (2022) 110319. 110319. https://doi.org/10.1016/j.celrep.2022.110319.

[34] C.A. Oliva, C. Montecinos-Oliva, N.C. Inestrosa, Wnt Signaling in the Central Nervous System: New Insights in Health and Disease, Progress in Molecular Biology and Translational Science. 153 (2018) 81-130. https://doi.org/10.1016/bs.pmbts.2017.11.018.

[35] Y. Zhang, X. Wang, Targeting the Wnt/β-catenin signaling pathway in cancer, Journal of Hematology & Oncology. 13 (2020) 165. https://doi.org/10.1186/s13045-020-00990-3.

[36] K. Minton, Pyroptosis heats tumour immunity, Nature Reviews Immunology. 20 (2020) 274-275. https://doi.org/10.1038/s41577-020-0297-2.

[37] H. Wu, X. Che, Q. Zheng, et al., Caspases: A Molecular Switch Node in the Crosstalk between Autophagy and Apoptosis, International Journal of Biological Sciences. 10 (2014) 1072-1083. https://doi.org/10.7150/ijbs.9719.

[38] Y. Han, X. Chen, H. Gao, et al., Physcion inhibits the metastatic potential of human colorectal cancer SW620 cells in vitro by suppressing the transcription factor SOX2, Acta Pharmacologica Sinica. 37 (2016) 264-275. https://doi.org/10.1038/aps.2015.115.

[39] M. Amin, T. Navidifar, S. Saeb, et al., Tumor-targeted induction of intrinsic apoptosis in colon cancer cells by Lactobacillus plantarum and Lactobacillus rhamnosus strains, Molecular Biology Reports. 50 (2023) 5345-5354. https://doi.org/10.1007/s11033-023-08445-x.

[40] R.X. He, B.Y. Jia, D.Y. Peng, et al., Caged Polyprenylated Xanthones in Garcinia hanburyi and the Biological Activities of Them, Drug Design Development and Therapy. 17 (2023) 3625-3660. https://doi.org/10.2147/dddt.S426685.

[41] Y. Lv, Y. Zhou, Z. Jin, et al., Structural characterization of galactomannan sulfated modification products with different molecular weight fractions and their in vitro anti-lung cancer activities, International Journal of Biological Macromolecules. 315 (2025) 144326. 144326. https://doi.org/10.1016/j.ijbiomac.2025.144326.

[42] M.G. Cerrito, E. Grassilli, Identifying Novel Actionable Targets in Colon Cancer, Biomedicines. 9 (2021) 579. https://doi.org/10.3390/biomedicines9050579.

[43] R.J. Youle, A. Strasser, The BCL-2 protein family: opposing activities that mediate cell death, Nature Reviews Molecular Cell Biology. 9 (2008) 47-59. https://doi.org/10.1038/nrm2308.

[44] M. Kvansakul, S. Caria, M.G. Hinds, The Bcl-2 Family in Host-Virus Interactions, Viruses. 9 (2017) 290. 290. https://doi.org/10.3390/v9100290.

[45] J.E. Park, Y. Seo, J.S. Han, HM-Chromanone Isolated from Portulaca Oleracea L. Protects INS-1 Pancreatic Cells against Glucotoxicity-Induced Apoptosis, Nutrients. 11 (2019) 404. https://doi.org/10.3390/nu11020404.

[46] N.T. Ha, C.H. Lee, Roles of Farnesyl-Diphosphate Farnesyltransferase 1 in Tumour and Tumour Microenvironments, Cells. 9 (2020) 2352. https://doi.org/10.3390/cells9112352.

[47] M. Kiani, M.S. Mehranjani, M.A. Shariatzadeh, Myoinositol improves sperm parameters in diabetic rats by reducing oxidative stress and regulating apoptosis-related genes, Journal of Molecular Histology. 56 (2025) 165. 165. https://doi.org/10.1007/s10735-025-10451-1.

[48] K.W. Sun, H.W. Li, Y. Dong, et al., The Use of Identified Hypoxia-related Genes to Generate Models for Predicting the Prognosis of Cerebral Ischemia-reperfusion Injury and Developing Treatment Strategies, Molecular Neurobiology. (2024) https://doi.org/10.1007/s12035-024-04433-9.

[49] K. Engeland, Cell cycle regulation: p53-p21-RB signaling, Cell Death and Differentiation. 29 (2022) 946-960. https://doi.org/10.1038/s41418-022-00988-z.

[50] L. Liu, S. Huang, M. Xu, et al., Isoquercitrin protects HUVECs against high glucose-induced apoptosis through regulating p53 proteasomal degradation, International Journal of Molecular Medicine. 48 (2021) 122. 122.

https://doi.org/10.3892/ijmm.2021.4955.

[51] Y.J. Zhang, Z.G. Xu, S.Q. Li, et al., Benzimidazoisoquinoline derivatives inhibit glioblastoma cell proliferation through down-regulating Raf/MEK/ERK and PI3K/AKT pathways, Cancer Cell International. 18 (2018) 90. https://doi.org/10.1186/s12935-018-0588-x.

[52] Z. Li, Q. Gao, Induction of apoptosis in HT-29 cells by quercetin through mitochondria-mediated apoptotic pathway, Animal Cells and Systems. 17 (2013) 147-153. https://doi.org/10.1080/19768354.2013.793210.

[53] M. Song, A.T. Chan, Environmental Factors, Gut Microbiota, and Colorectal Cancer Prevention, Clinical Gastroenterology and Hepatology. 17 (2019) 275-289. https://doi.org/10.1016/j.cgh.2018.07.012.

[54] N.T. Baxter, J.P. Zackular, G.Y. Chen, et al., Structure of the gut microbiome following colonization with human feces determines colonic tumor burden, Microbiome. 2 (2014) 20. 20. https://doi.org/10.1186/2049-2618-2-20.

[55] A. Merlos, P. Rodriguez, I. Barcena-Uribarri, et al., Toxins Secreted by Bacillus Isolated from Lung Adenocarcinomas Favor the Penetration of Toxic Substances, Frontiers in Microbiology. 6 (2015) 1301. https://doi.org/10.3389/fmicb.2015.01301.

[56] A. Singh, S.V. Chandrasekar, V.T. Valappil, et al., Tumor immunomodulation by nanoparticle and focused ultrasound alters gut microbiome in a sexually dimorphic manner, Theranostics. 15 (2025) 216-232. https://doi.org/10.7150/thno.99664.

[57] H. Hua, Y. Sun, X. He, et al., Intestinal Microbiota in Colorectal Adenoma-Carcinoma Sequence, Frontiers in Medicine. 9 (2022) 888340. 888340. https://doi.org/10.3389/fmed.2022.888340.

[58] J. Xie, Y. Liu, B. Chen, et al., Gonoderma lucidum polysaccharide improves rat DSS-induced colitis by altering cecal microbiota and gene expression of colonic epithelial cells, Food & Nutrition Research. 63 (2019) 1559. 1559. https://doi.org/10.29219/fnr.v63.1559.

[59] X. Zhang, B. Zhang, B. Peng, et al., Different Dose of Sucrose Consumption Divergently Influences Gut Microbiota and PPAR-γ/MAPK/NF-κB Pathway in DSS-Induced Colitis Mice, Nutrients. 14 (2022) 2765. 2765. https://doi.org/10.3390/nu14132765.

[60] C. Zhang, N. Zhang, Y. Zhang, et al., Effects of Lactobacillusplantarum-loaded W1/O/W2 emulsions stabilized by ultrasonically treated pea protein on DSS-induced colitis in mice, International Journal of Biological Macromolecules. 311 (2025) 143956. 143956. https://doi.org/10.1016/j.ijbiomac.2025.143956.

[61] B.H. Sajer, W.A. Alshehri, S.S. Alghamdi, et al., Aspergillus Species from the Sabkha Marsh: Potential Antimicrobial and Anticancer Agents Revealed Through Molecular and Pharmacological Analysis, Biologics: Targets and Therapy. 18 (2024) 207-228. https://doi.org/10.2147/btt.S472491.

[62] A. Viggiano, O. Salo, H. Ali, et al., Pathway for the Biosynthesis of the Pigment Chrysogine by Penicillium chrysogenum, Applied and Environmental Microbiology. 84 (2018) e02246-02217. e02246-17. https://doi.org/10.1128/aem.02246-17.

[63] Y. Gao, P. Zens, M. Su, et al., Chemotherapy-induced CDA expression renders resistant non-small cell lung cancer cells sensitive to 5′-deoxy-5-fluorocytidine (5′-DFCR), Journal of Experimental & Clinical Cancer Research. 40 (2021) 138. 138. https://doi.org/10.1186/s13046-021-01938-2.

[64] C. Wolf, M. Bruess, B. Haenisch, et al., Molecular basis for the antiproliferative effect of agmatine in tumor cells of colonic, hepatic, and neuronal origin, Molecular Pharmacology. 71 (2007) 276-283. https://doi.org/10.1124/mol.106.028449.

[65] T.Y. Lee, Y.H. Kim, S.W. Yoon, et al., Oral administration of poly-gamma-glutamate induces TLR4-and dendritic cell-dependent antitumor effect, Cancer Immunology Immunotherapy. 58 (2009) 1783-1796. https://doi.org/10.1007/s00262-009-0689-4.